

WARM GAS AROUND AGB STARS

I. Yamamura^{1,2} and T. de Jong^{2,3}

¹Laboratory of Infrared Astrophysics, ISAS, Yoshino-dai 3-1-1, Sagamihara, 229-8510 Kanagawa, Japan

²Astronomical Institute ‘Anton Pannekoek’, University of Amsterdam, Kruislaan 403, 1098 SJ, Amsterdam, the Netherlands

³SRON-Utrecht, Sorbonnelaan 2, 3584 CA Utrecht, the Netherlands

ABSTRACT

The impact of the ISO/SWS on the study of AGB stars is reviewed. The ISO/SWS has provided high quality, intermediate resolution spectra covering a wide infrared wavelength range. These data enable us, for the first time, to perform an extensive study of the outer atmosphere and inner circumstellar regions of AGB stars. Many new and unexpected features hidden by the terrestrial atmosphere are detected, which raise new questions. We here particularly focus on the detection of dioxides in the O-rich stars, of C₃, C₂H₂, and HCN in carbon stars, and of atomic / ionic fine-structure lines. We discuss the interpretation of these results and list problems to be solved.

Key words: Stars: AGB and post-AGB – Stars: atmospheres – Stars: late-type – Infrared: stars

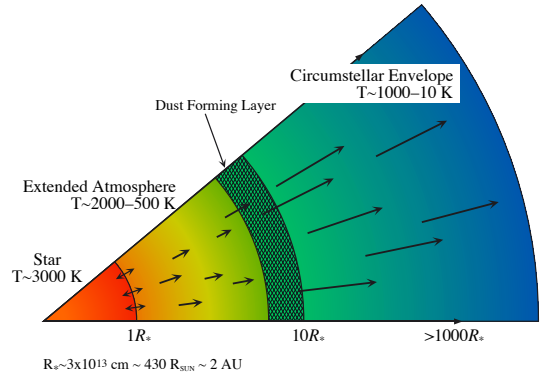


Figure 1. A schematic view of the AGB star atmosphere. Stellar pulsations drive material from the surface into the so-called extended atmosphere. The matter slowly moves outward into the extended atmosphere, and when the gas temperature falls below about 1000 K, dust grains may form. Strong radiation pressure on the dust by the central star blows the matter out into the circumstellar envelope.

1. INTRODUCTION

The AGB (Asymptotic Giant Branch) is the last evolutionary stage of low- to intermediate-mass stars ($1 M_{\odot} \leq M_{\star} \leq 8 M_{\odot}$). In the AGB phase, stars are red-giants with effective temperatures of typically 3000 K and radii of several hundred R_{\odot} , corresponding to luminosities of several times 10^3 – $10^4 L_{\odot}$. Quite often AGB red-giants are observed as variable stars of Mira or semi-regular type. Miras may vary in the visual wavelengths by several magnitudes with periods of typically one year.

The most conspicuous feature of AGB stars is their mass loss, with the rates in the range 10^{-7} – $10^{-4} M_{\odot} \text{ yr}^{-1}$. Mass loss affects the evolution of the stars themselves, and also the chemical evolution of galaxies. It is generally believed that stellar pulsation plays an important role in driving the mass-loss. Figure 1 shows a schematic view of the vicinity of an AGB star. The matter on the surface of the star is pushed up by pulsations. If the pulsation is periodic and strong enough, matter is transported outwards by subsequent pulsations. Further out in the flow, gas cools down enough so that dust grains can form. Radiation pressure from the central star on the dust blows the material out into the circumstellar envelope and eventually out into interstellar space.

Though its importance has been recognized, our understanding of the pulsation dominated region between the

stellar surface (photosphere) and the circumstellar envelope (dust forming region), the so-called *extended atmosphere*, has until recently been largely based on theoretical studies. Near- and mid-infrared spectroscopy provides the best tools to probe this region. Space-borne observations with ISO for the first time allowed a systematic study of this wavelength region that is usually obscured by the earth’s atmosphere. Especially, thanks to its relatively high-resolution, the SWS has enabled us to study the molecular gas in the extended atmosphere. In this paper, we review the ISO/SWS spectra of AGB stars (section 2), summarize the new discoveries (section 3), and discuss the possible interpretation of these new observational data (section 4).

2. ISO/SWS SPECTRA OF AGB STARS

Figure 2 shows representative ISO/SWS spectra of O-rich and C-rich AGB red-giants with relatively low mass-loss rates. The nature of AGB stars is primarily determined by the C/O abundance ratio. Since almost all available carbon or oxygen atoms are locked into the very stable molecule CO, either C or O which remains will dominate the molecular chemistry. In the oxygen-rich atmosphere, SiO, OH, H₂O, etc. are expected to be abundant (Tsuji

1964; Tsuji 1973). These species are clearly detected in the ISO/SWS spectrum of R Cas. Dust emission of amorphous silicates with some additional substructure is also observed. On the other hand, CN, C₂, C₃, C₂H₂, and HCN are expected in the atmospheres of carbon stars. In the ISO/SWS spectral range, HCN, C₂H₂, and C₃ show strong absorption features as observed in R Scl.

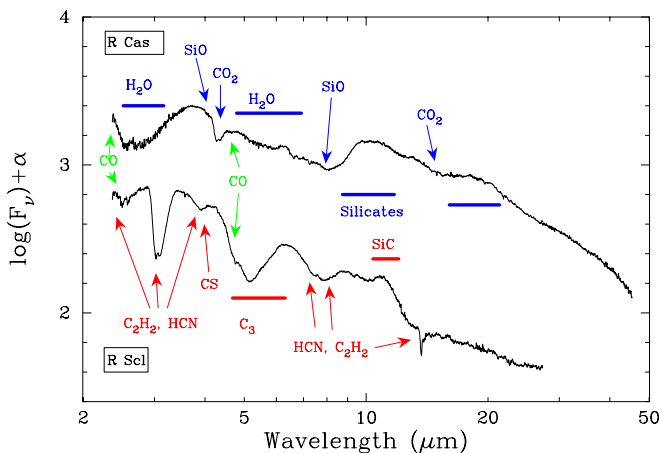


Figure 2. Representative ISO/SWS spectra of two AGB stars. The spectrum of the oxygen-rich star R Cas is dominated by the molecular features of H₂O, SiO, CO₂, etc., while that of the carbon-rich star R Scl shows strong bands of carbon-bearing molecules such as C₂H₂, HCN, C₃ etc.

3. ISO'S DISCOVERY

3.1. OXYGEN-RICH STARS

One of the most unexpected discoveries made by the ISO/SWS in the spectra of AGB stars is the detection of dioxide molecules. In particular, the detection of warm SO₂ gas was a surprise. The ν_2 ro-vibration band at 7.3 μm is clearly detected in three stars out of 10 O-rich stars studied by Yamamura et al. (1999a) (Figure 3). We afterwards also found this band in the archived data of quite a few stars. This indicates that the phenomenon is rather normal in this type of stars. The band is seen either in emission or absorption. One of the stars studied by Yamamura et al. (1999a), T Cep, showed the time variation of the feature. It is particularly interesting that this variation does not correlate with the visual variability. The band is seen in emission at the first minimum, while it is in absorption in the next minimum. Unfortunately, the ISO mission only covered 1.4 period of the star, and it is not clear whether this variation is a transient phenomenon or it has a multi-periodicity of the pulsation cycle. From a simple analysis using a *thermal slab* model, Yamamura et al. (1999a) concluded that the molecule is located typically at 5 R_{*} in T Cep with a temperature of 600 K. The time variation

can be explained if the molecular layer (effectively) shrinks with the time.

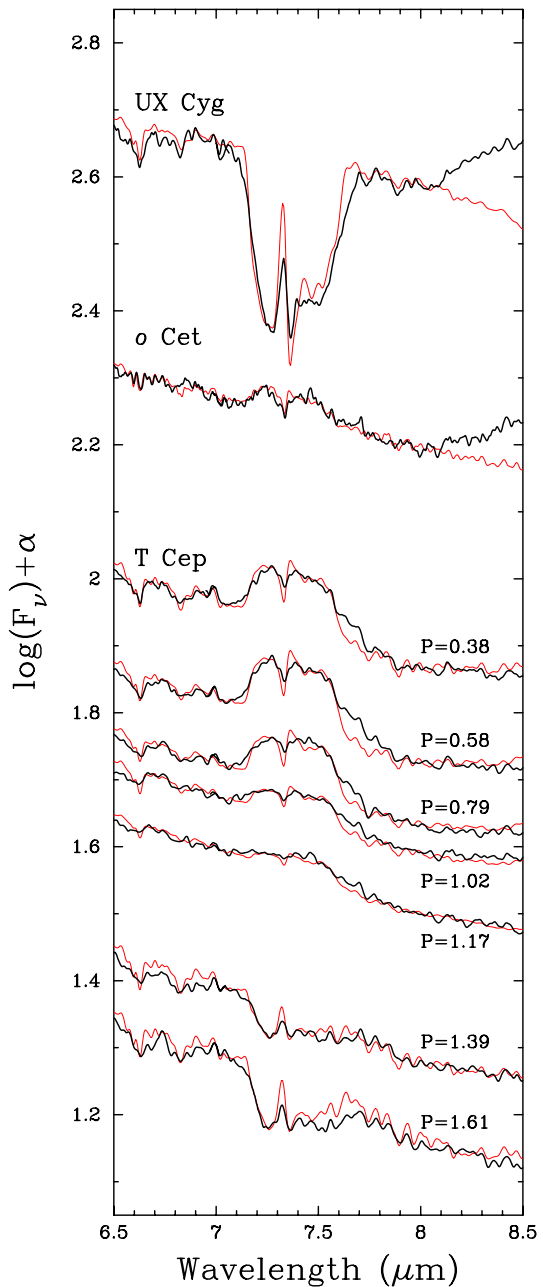


Figure 3. The SO₂ ν_3 band at 7.3 μm in three O-rich Miras (black line). The band is seen either in emission or absorption. The spectra of T Cep show that the feature changes from emission to absorption in about one year. However, the variation does not follow the optical period, indicated in the figure. A thermal slab model fits the observed features satisfactorily (red line). This figure is taken from Yamamura et al. (1999a).

The presence of CO₂ around O-rich AGB stars has been expected before the ISO observations. Willacy & Millar (1997) showed that the CO₂ may be as abundant as

10^{-7} at a few hundred R_{\star} following the photodissociation of H_2O into OH and the subsequent reaction with CO. However, the ISO/SWS observations showed that CO_2 is already abundant in the extended atmosphere of these stars. Warm CO_2 gas of several hundred K appears both in the $4.3 \mu\text{m}$ and the $15 \mu\text{m}$ regions. Especially interesting is that some O-rich stars with relatively low mass-loss rates (stars with so-called “ $13 \mu\text{m}$ ” dust features; Onaka, de Jong, & Willems 1989; Posch et al. 1999) exhibit satellite bands at 13.9 , 15.4 , $16.2 \mu\text{m}$, etc. prominently (Justanont et al. 1998; Ryde, Eriksson, & Gustafsson 1999). These satellite bands arise from excited vibrational levels and are always seen in emission, in contrast to the fundamental band at $15.0 \mu\text{m}$, which is sometimes seen in absorption. The intensities of the satellite bands cannot be explained by a single temperature molecular layer. Using a simple thermal slab model, Cami et al. (2000) argue that the molecules are distributed in the extended atmosphere and circumstellar shell (say, $R \sim 4\text{--}10 R_{\star}$) with temperatures in the range $100\text{--}700$ K, and they show that the lines are optically thick. Radiative pumping has been discussed by González-Alfonso & Cernicharo (1999). They pointed out that dust emission may increase the efficiency of the radiative pumping significantly.

Different molecules probe different regions in the extended atmosphere. Yamamura et al. (1999b) analyzed near-infrared H_2O bands in two Mira variables using a thermal slab model. They demonstrated that the observed spectra are reasonably well fitted by two H_2O layers with temperatures of 2000 K and $1200\text{--}1400$ K, respectively. We note that this does not directly mean that there are two distinct layers in the atmosphere of these stars. Two layers may just represent density/temperature gradients in the atmosphere. Yamamura et al. (1999b) found that the size of the H_2O layers is $1\text{--}3 R_{\star}$: smaller than that of dioxide molecules. In some cases (e.g. *o* Cet) the 2000 K layer extends as large as $2 R_{\star}$, and the molecular band is seen in emission.

In Figure 4, we show the seven spectra of T Cep in the $2.3\text{--}5.3 \mu\text{m}$ region. The shape of the H_2O bands seems to repeat (though not perfectly) after one cycle, i.e. the H_2O layers near the photosphere seem to follow the stellar pulsation. A detailed analysis of the time variation of the near-infrared H_2O bands is in progress (Matsuura et al. 2000).

3.2. CARBON-RICH STARS

The ISO/SWS spectra of carbon stars are dominated by polyatomic molecules such as C_2H_2 , HCN, and C_3 . The $5.2 \mu\text{m}$ band has been attributed to $\text{C}_3 \nu_1 + \nu_3$ combination band with a contribution from the ν_2 bending-mode (Treffers & Gilra 1975). It is very interesting that the band is clearly observed only in visual carbon stars with low mass-loss rates (say, $\dot{M} \leq 10^{-7} M_{\odot} \text{yr}^{-1}$), while it almost disappears when the mass-loss rate exceeds about

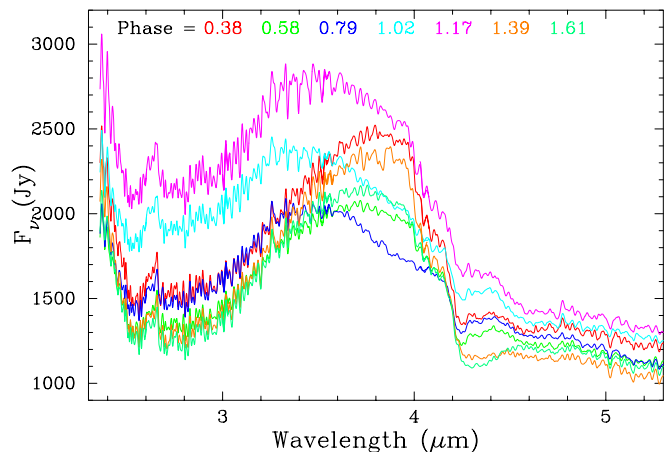


Figure 4. Time variation of the SWS spectra of T Cep. The optical phases at the observations are indicated at the top of the plot. The spectra in this wavelength region are dominated by the H_2O absorption band centered around $2.7 \mu\text{m}$. The CO ($4.6 \mu\text{m}$ and $2.3 \mu\text{m}$), SiO ($4.1 \mu\text{m}$), and CO_2 ($4.3 \mu\text{m}$) bands are clearly detected. Sharp absorption lines between $3.0\text{--}3.5 \mu\text{m}$ are due to OH.

$10^{-6} M_{\odot} \text{yr}^{-1}$ (Yamamura et al. 1998). This is not due to obscuration by circumstellar dust, since other molecular features in the near-infrared wavelengths are still clearly recognized in these intermediate mass-loss rates stars. The fact that the visual carbon stars in the sample of Yamamura et al. (1998) are all semi-regular variables, while the other stars are Miras, strongly implies that the difference is caused by a change in their atmospheric structure related to the pulsation.

Both C_2H_2 and HCN have transitions at wavelengths of $3 \mu\text{m}$, $7 \mu\text{m}$, and $14 \mu\text{m}$. Especially the $14 \mu\text{m}$ region is interesting because it is only observable from space. A beautiful illustration of molecular physics is observed in the $14 \mu\text{m}$ region. A narrow emission feature is often seen at $14.3 \mu\text{m}$ in the spectra of carbon stars (Figure 5; Cernicharo et al. 1999; Aoki, Tsuji, & Ohnaka 1999), due to the Q-branch of the HCN $\nu_2 = 2^0 \rightarrow 1^1$ transition. The band is very likely excited radiatively. Excitation from the ground-state to the ν_2 level by absorption of photons at $7 \mu\text{m}$ is only allowed to $\nu_2 = 2^0$, which eventually are re-emitted in the $14.3 \mu\text{m}$ band. Detailed radiative transfer calculations by González-Alfonso & Cernicharo (1999) show that most of the transitions including ν_2 should also be seen in emission, though strong contamination by C_2H_2 and HCN itself prevents a clear detection. It is interesting that although C_2H_2 also has such a radiative excitation path, we only see absorption bands for this molecule. On the other hand, HCN $14.3 \mu\text{m}$ emission is very often observed regardless of mass-loss rate. More complicated physical and chemical processes may be required to explain the difference between two molecules.

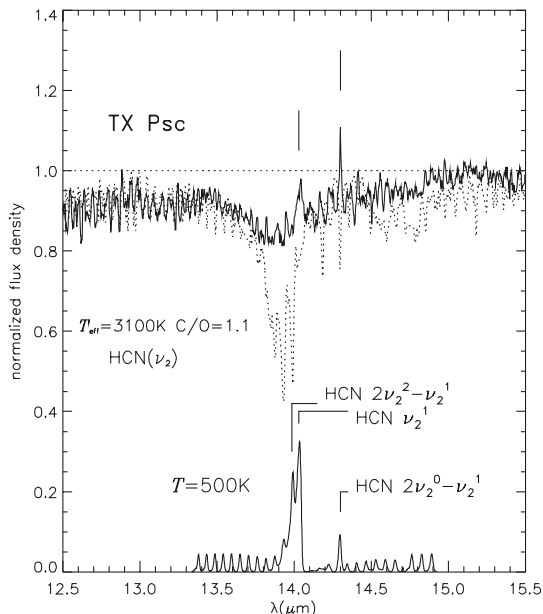


Figure 5. The HCN emission bands in TX Psc. The $14.3 \mu\text{m}$ bands are likely excited by the radiative pumping via $2\nu_2^0$ level by $7 \mu\text{m}$ photons. (taken from Aoki et al. 1999)

3.3. Atomic / ionic lines

Aoki, Tsuji, & Ohnaka (1998a) have reported the detection of fine-structure emission lines in the spectra of both O-rich and C-rich stars. These lines are observed in relatively early, low mass-loss rate stars. They found that lines of neutral species, [Fe I] ($24.042 \mu\text{m}$) and [Si I] ($25.249 \mu\text{m}$) are detected in carbon stars (TX Psc and WZ Cas), while lines from ionized species, [Si II] ($34.814 \mu\text{m}$) and [Fe II] ($35.349 \mu\text{m}$) are observed in the O-rich giant, 30g Her. The [Fe II] line at $25.988 \mu\text{m}$ is detected in both stars. Although the sample is small (three stars), they speculated that the result indicates differences in the stellar atmospheres of the two types of stars. According to their analysis, the lines arise from warm, dense gas with temperatures of several hundred K and densities of the order of 10^9 cm^{-3} , in the extended atmosphere.

Justtanont et al. (1999) reported the detection of [Fe II] and [Si II] in α Ori and α Sco. In the case of these red super-giants, the lines arise from the region inside of the dust forming region, with temperatures of 1200–1800 K. The energy budget, mass of the emitting gas, and the source of photon ionization are rather well reproduced by existing models for these stars. In contrast, such detailed models are not available for the AGB giants. Their ionization/excitation sources are not clear. If they arise from the warm gas layer in the atmosphere as Aoki, Tsuji, & Ohnaka (1998a) suggested, their co-existence with neutral molecules ought to be explained

4. Interpretation

4.1. Physical conditions

Spherical, hydrostatic model atmospheres have been used to analyze SWS spectra of many non-Mira variables. These semi-regulars or irregular variables are thought to have much less periodic and lower pulsation amplitude variations, and thus do not develop extended atmospheres. For example, Aoki, Tsuji, & Ohnaka (1998b) demonstrated that the difference in the spectra of SC- and N-type carbon stars can be explained in terms of their C/O ratio and their effective temperature, using hydrostatic model. We note that the spectral responsivity calibration of the SWS itself has been evaluated using the hydrostatic model atmospheres, especially at short wavelengths (Decin et al. 2000, this proceedings).

However, even in these relatively quiescent stars, there are often obvious deviations between the model spectra and the SWS observations. Tsuji et al. (1997) detected the $2.7 \mu\text{m}$ absorption band of water vapor in the M2 irregular variable β Peg, which is not expected from their hydrostatic model ($T_{\text{eff}} = 3600 \text{ K}$). They also detected the CO_2 band at $4.3 \mu\text{m}$ in M6 and M7 semi-regulars. The molecules have an excitation temperature of roughly 1000 K, and are thought to be located at $2 R_\star$ or beyond. Loidle et al. (2000, this proceedings) show that the hydrostatic model spectrum reasonably represents the near-infrared part of the SWS spectrum of the irregular variable carbon star TX Psc. However, the broad $14 \mu\text{m}$ band of C_2H_2 and HCN in their model spectrum is too deep compared to the observed spectrum. These results indicate the presence of additional extra matter above the hydrostatic photosphere and/or the importance of some physical processes not included in the present hydrostatic models.

The spectra of Mira variables are not well fitted by hydrostatic model atmospheres. Contributions from the outer layers dominate the observed spectrum, as we showed in the previous section. Time-dependent model atmospheres taking account of stellar pulsation have been developed (Bowen 1988; Fleischer, Gauger & Sedlmayr 1991; Bessell, Scholz, & Wood 1996; Höfner et al. 1998). These models have been rather successful for the case of carbon stars, for which the molecular chemistry and the dust formation process are better understood. Hron et al. (1998) and Loidl et al. (1999) have shown that the time variation of the infrared spectra of R Scl¹ is qualitatively reproduced by synthesized spectra based on the dynamical model atmosphere. Recent progress in this area is reviewed by Höfner et al. (2000), Aringer et al. (2000), and Loidl et al. (2000) in this proceedings.

It is not clear whether the dynamical model atmosphere is the general framework to understand the atmo-

¹ R Scl is classified as semi-regular variable but the star shows rather periodic and large visual amplitude of ~ 2.5 mag, which is comparable to Miras.

spheres of AGB stars, including semi-regular or irregular variables. The *warm gas layer* in non-Mira variables reported by Tsuji et al. (1997) and Aoki, Tsuji, & Ohnaka (1998a) has rather high density, while the visual amplitudes of the stars are in the range 0.3–2.0 mag. This problem has not been investigated in detail and is encouraged to be studied. We note that Loidle et al. (2000, this proceedings) show that inclusion of weak pulsation can improve the fit of the 14 μm band in the spectrum of TX Psc, though side-effects appears in the short wavelengths.

Dynamical model atmospheres have not been used to fit O-rich Miras except works by Aringer et al. (1999; 2000, this proceedings). Yamamura et al. (1999a,b) and Cami et al. (2000) have analyzed the spectra using a simple LTE *slab* model. The model consists of a blackbody background star with molecular layer(s) on top of it. The molecular layer with a constant column density is allowed to extend beyond the size of the background star, so that an extra emission contributes to the spectrum. Despite the simplicity of this approach, the results of the modeling (the column density, excitation temperature, and size of the molecular layer) are useful to obtain some insight in the complicated nature of the extended atmospheres.

Model (Höfner et al. 1998, A&A 340, 497, Fig. 9) vs. Observations

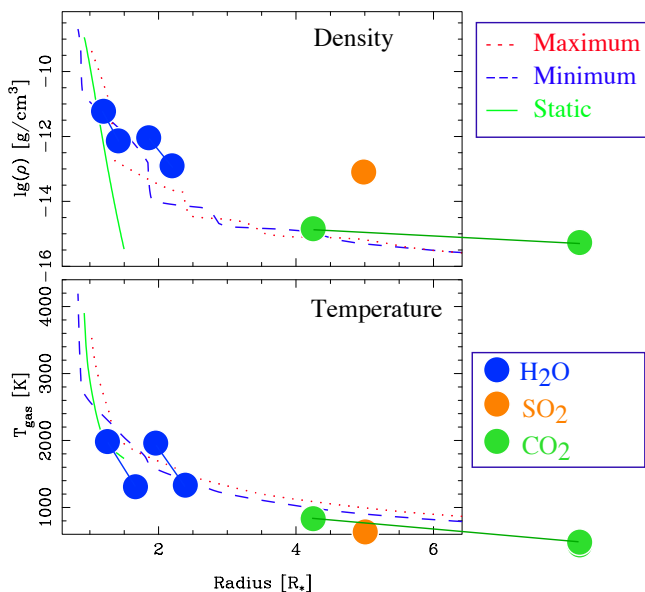


Figure 6. The local gas density and temperature derived for different molecules by the thermal slab model are compared with the theoretical calculations by Höfner et al (1998). Circles connected by lines are derived from the same star. The results of model analysis are reasonably consistent with the theoretical prediction, except that the density derived from SO_2 is too high. No velocity information is available from the SWS.

Figure 6 compares the estimated local density and temperature of molecular layers using three different molecules as probes, with results from theoretical calculations of dynamical atmospheres by Höfner et al. (1998). This comparison shows that the results from H_2O and CO_2 are reasonably consistent with the models. Because of the oversimplified nature of the model analysis and the limited size of the stellar sample analyzed so far, it is not possible to conclude on the effects of the time variation of the parameters.

4.2. Excitation

In the most calculations of synthesized spectra, the molecules are assumed to be in local thermodynamic equilibrium (LTE). As the gas moves outwards and the density decreases, the excitation may start to deviate from LTE. Woitke et al. (1999) indicate that the vibrational temperature is expected to deviate from LTE already rather close to the photosphere. The rotational temperature may be close to LTE out to about two stellar radii. The vibrational temperature is generally related to the absolute intensity of the band via the level populations, while the rotational temperature determines the shape of the bands. Differences between these two temperatures complicate the model analysis. However, our recent explanatory non-LTE calculations of multi-level radiative transfer of CO_2 molecules suggests that both the vibrational and the rotational levels of CO_2 remain about thermalized out to about five stellar radii.

A clear example of the importance of radiative pumping is the HCN 14.3 μm bands. However, in general, it is not easy to estimate the importance of non-LTE effects on the excitation of particular molecules, since the formation of the molecular lines depends on the density, temperature, and velocity structure in the region. Lack of accurate collisional cross-sections for ro-vibrational transitions is another cause of uncertainty.

4.3. Chemistry

The detection of SO_2 and CO_2 in the atmospheres of AGB stars is one of the big surprises discovered by the ISO/SWS. These molecules are not expected to be abundant according to thermal equilibrium calculations (Tsuji 1964; Tsuji 1973). The SO_2 abundance in thermal equilibrium is expected to be less than 10^{-10} . Although it is difficult to derive an accurate abundance from the ISO/SWS data, the detection of strong SO_2 band indicates that a significant fraction of sulfur atoms must be in the form of SO_2 . The CO_2 abundance is probably also enhanced by at least a few orders of magnitude.

These facts of course imply that non-equilibrium chemical processes dominate the chemical structure in the extended atmosphere. Duari, Cherchneff, & Willacy (1999) recently showed that non-equilibrium chemistry in pulsa-

tion shocks may enhance the abundance of some carbon-bearing molecules in the O-rich atmospheres. Beck et al. (1992) found that non-equilibrium chemical processes increase the SO₂ abundance significantly, if UV radiation from the central star is suppressed. Further detailed modeling of the ISO data is urgently required.

4.4. Time variation

As mentioned in the previous section, the time variation of the molecular features in O-rich Mira variables is complicated. It is remarkable that the SO₂ band in T Cep does not follow the pulsation period. Unfortunately, the ISO/SWS observations covers only 1.4 period and thus it is impossible to conclude whether this is a transient phenomenon or whether it repeats with a longer period related to the optical variation. CO₂ bands also seem to vary at a longer time scale than the optical period (Figure 4). On the other hand, the shape of the near-infrared H₂O band roughly repeats after one cycle. Together with the fact that the dioxide molecules are located far from the central star whereas the H₂O band is formed within a few stellar radii, we conclude that the extended atmospheres in Mira variables can be divided observationally into two regions. The inner part ($R \lesssim 3 R_{\star}$) follows stellar pulsation, and the molecular abundances are explained by thermal equilibrium. In the outer region the variation does not follow the stellar pulsation anymore, and the non-thermal chemistry dominates the chemical structure.

5. Summary

ISO/SWS spectra of AGB stars have significantly increased our understanding of the extended atmospheres of the AGB stars. The full wavelength coverage of the ISO/SWS has enabled us to detect many unexpected features and to make a comprehensive study of the subject.

One very important piece of information not provided by the SWS data is the velocity. To further improve our understanding of the extended atmosphere, velocity information is essential. Such information has been available from the high-resolution spectrograph using ground-base telescopes (e.g., Hinkle, Lebzelter, & Scharlach 1997). These data are almost exclusively taken in the K-band and at shorter wavelengths, and thus probe the region close to the photosphere. In future space missions, high-resolution spectra of molecular features at longer infrared wavelengths are essential for the investigation of the outer part of the extended atmosphere and the dust forming processes.

The analysis of the ISO/SWS spectra has just started. We stress the importance of the basic input parameters for the models: complete and accurate molecular line list, collisional cross section for ro-vibrational transitions, etc. of many molecules.

ACKNOWLEDGEMENTS

The authors acknowledge to M. Matsuura for careful reading of the manuscript and discussions.

REFERENCES

- Aoki W., Tsuji T., Ohnaka K., 1998a, A&A 333, L22
Aoki W., Tsuji T., Ohnaka K., 1998b, A&A 340, 222
Aoki W., Tsuji T., Ohnaka K., 1999, A&A 350, 945
Aringer B., Höfner S., Wiedemann G., et al., 1999, A&A 342, 799
Aringer B., Kerschbaum F., Hron J., Höfner S., 2000, this proceedings
Beck H.K.B., Gail H.-P., Henkel R., Sedlmayr E., 1992, A&A 265, 626
Bessell M.S., Scholz M., Wood P.R., 1996, A&A 307, 481
Bowen G.H., 1988, ApJ 329, 299
Cami J., Yamamura I., de Jong T., et al., 2000, in preparation
Cernicharo J., Yamamura I., González-Alfonso E., et al., 1999, ApJ 526, L41
Decin L., Wealkens C., Eriksson K., et al., 2000, this proceedings
Duari D., Cherchneff I., Willacy K., 1999, A&A 341, L47
Fleischer A.J., Gauger A., Sedlmayr E., 1991, A&A 242, L1
González-Alfonso E., Cernicharo J., 1999, In: P. Cox, M.F. Kessler (eds.), The Universe as seen by ISO, ESA SP-427, Noordwijk, p.325
Hinkle K.H., Lebzelter T., Scharlach W.W.G., 1997, AJ 114, 2686
Höfner S., Jørgensen U.G., Loidl R., Aringer B., 1998, A&A 340, 497
Höfner S., Loidl R., & Aringer B., Jørgensen U.G., Hron J., 2000, this proceedings
Hron J., Loidl R., Höfner S., et al., 1998, A&A 335, L69
Justtanont K., Feuchtgruber H., de Jong, T., et al., 1998, A&A 330, L17
Justtanont K., Tielens A.G.G.M., de Jong, T., et al., 1999, A&A 345, 605
Loidl R., Höfner S., Jørgensen U.G., Aringer B., 1999, A&A 342 531
Loidl R., Hron J., Jørgensen U.G., Höfner S., 2000, this proceedings
Matsuura M., Yamamura I., de Jong T., et al., 2000, in preparation
Onaka T., de Jong T., Willems F.J., 1989, A&A 218, 169
Posch T., Kerschbaum F., Mutschke H., et al., 1999, A&A 352, 609
Ryde N., Eriksson K., Gustafsson B., 1999, A&A 341, 579
Treffers R.R., Gilra D.P., 1975, ApJ 202, 839
Tsuji T., 1964, Ann. Tokyo Astron. Obs., 2nd Ser. 9, 1
Tsuji T., 1973, A&A 23, 411
Tsuji T., Ohnaka K., Aoki W., Yamamura I., 1997, A&A 320, L1
Willacy K., Millar T.J., 1997, A&A 324, 237
Woitke P., Helling Ch., Winters J.M., & Jeong K.S., 1999, A&A 348, L17
Yamamura I., de Jong T., Justtanont K., et al., 1998, ApSS 255, 351
Yamamura I., de Jong T., Onaka T., et al., 1999a, A&A 341, L9
Yamamura I., de Jong T., Cami J., 1999b, A&A 348, L55